Journal of Catalysis 260 (2008) 30–36

Contents lists available at ScienceDirect

Journal of Catalysis

www.elsevier.com/locate/jcat

Effect of several cationic substitutions in the *M1* active phase of the MoVTeNbO catalysts used for the oxidation of propane to acrylic acid

B. Deniau [a], J.M.M. Millet [a,*], S. Loridant [a], N. Christin [a], J.L. Dubois [b]

[a] *Institut de Recherches sur la Catalyse et l'Environnement de Lyon, IRCELYON, UMR5256 CNRS-Université Claude Bernard Lyon 1, 2 avenue A. Einstein, F-69626 Villeurbanne cedex, France*
[b] *Arkema France, 420 Rue d'Estienne d'Orves, 92705 Colombes*

ARTICLE INFO

Article history:
Received 24 June 2008
Revised 26 August 2008
Accepted 26 August 2008

Keywords:
Propane oxidation and ammoxidation
M1-phase
MoVTeNb oxide catalysts
Substitution
XRD

ABSTRACT

Several cationic substitutions with Ti, Sn, Ge and W have been made in the *M1* active phase of the MoVTe(Sb)NbO catalysts in order to improve their catalytic properties for the partial oxidation of propane into acrylic acid. The catalysts were characterized by BET, XRD and chemical analysis and were studied for propane oxidation. The results obtained show that these substitutions were possible but remain limited. It was noted that Ge increased the activity of the *M1* phase whereas W maintained it and Ti and Sn decreased it. Concomitantly the selectivity to acrylic acid was slightly increased or decreased. The effect of Ge, which did not enter into the structure of the *M1* phase has been related to an increase of the vanadium content of the *M1* phase which occurs because of the formation of new Ge containing species in the slurry during the preparation of the catalyst.

1. Introduction

New multicomponents molybdates MoVTe(Sb)NbO have been proposed in the early 90's as efficient catalysts for the ammoxidation and oxidation of propane respectively into acrylonitrile and acrylic acid [1,2]. Since that time many authors have reported on these catalysts describing many aspects of their characterization such as the structure of the phases present in the catalysts [3–6], their role in the catalytic reaction [7] and the reaction mechanism [8–11]. The different elements constituting the active phase called *M1* have been characterized in terms of cationic environment and oxidation state [12–14], methods of synthesis have been described [15,16] as well as applications to other reactions such as the oxidative dehydrogenation of ethane [17,18] or oxidation of isobutane [19].

The active phase *M1* is a solid solution containing the four metallic cations with the total formula reported $(AO)_{2-2x}(A_2O)_x$-$M_{20}O_{56}$ with A = Te or Sb and M = Mo, V, Nb and $0 \leqslant x \leqslant 1$. The V/Mo and Nb/Mo ratios can vary, but are most frequently close to 0.3 and 0.1, respectively [13,14]. The structure is built up using 11 corner-sharing MO6 (M = Mo or V) octahedra forming pentagonal, hexagonal and heptagonal channels (*M1* to *M11* in Fig. 1). The heptagonal channels are empty, the hexagonal channels are partially occupied by (Te–O) or (Sb–O) chains and the pentagonal channels are fully occupied by Nb cations and oxygens. This last structural feature may better be described as {(Nb)Mo5} columns running in the 001 direction and constituting the skeleton of the structure [13,16].

Besides this phase, another phase called *M2* is generally formed when the catalysts are prepared. The phase is inactive to convert propane but can efficiently oxidize propene to acrylic acid leading to a synergetic effect when it is present with the *M1* phase in the catalysts [20–22]. However this effect only takes place when the catalysts contain tellurium and not when they contain antimony [23] and is not sufficient enough to allow the catalysts to compete with the industrialized process to produce acrylic acid. One way to try to improve the activity of these catalysts is to make substitutions in the *M1* phase. Te or Sb are located in the hexagonal channels of the structure and have 3 or 4 coordination which render them difficult to substitute. One study has been published on the substitution of tellurium or antimony cations by cesium cations [23]. The activity of the catalysts obtained was lower. Further attempts to reduce the cesium content after synthesis or to concomitantly substitute Mo and V cations by other metallic cations such as Ta, Nb, Bi or W during synthesis did not allow increasing significantly the activity. Moreover the selectivity to acrylic acid was very low because of difficulties in achieving the step of the oxidative transformation of propene to acrolein on such catalysts [23].

The substitution of only Mo, V or Nb, which exhibit more or less distorted octahedral coordination, should be easier. However, only one study dealing with such substitution has been published

* Corresponding author.
E-mail address: jean-marc.millet@ircelyon.univ-lyon1.fr (J.M.M. Millet).

0021-9517/$ – see front matter
doi:10.1016/j.jcat.2008.08.020

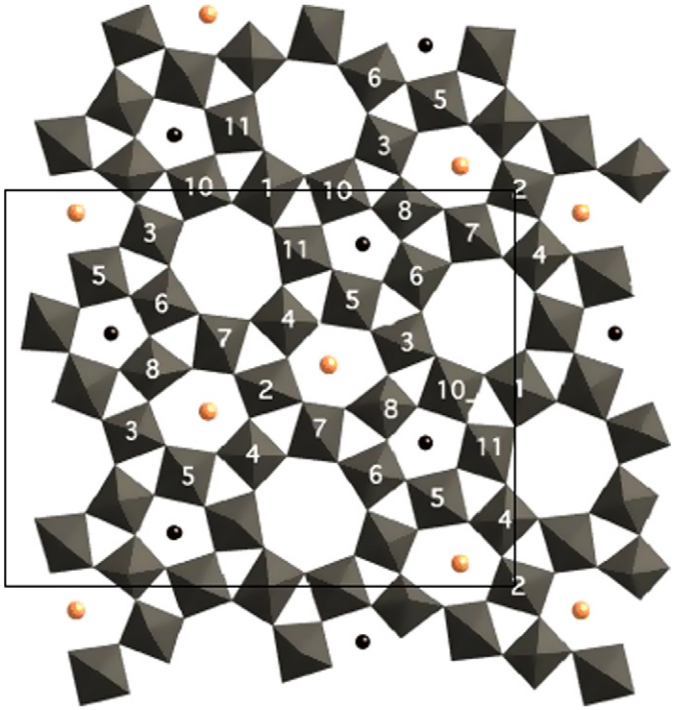

Fig. 1. Schematic representation of the basal plane (001) of *M1* phase of MoVNbTeO catalysts. Nb and Te cations are respectively colored in black and light gray. The MO6 octahedra are in gray. The oxygens bounded to the Nb and Te cations in the pentagonal and hexagonal channels are not reported for the clarity of the schema.

Table 1
Cationic sizes (pm) of the *M1* phase constituting elements and of the substituting ones selected for the study in octahedral coordination as a function of there valence state.

Valence state	V	Mo	Nb	W	Mn	Re	Ti	Ge	Sn
7+					60	67			
6+		73		74					
5+	68	75	78	76					
4+	72						74.5	67	83

[24]. It claimed that Nb cations could be substituted by Fe cations. The substitution, which was possible only when starting ferrous precursor was used for the preparation, did not improve the catalytic properties of the catalysts. Finally it can be reported that substitution in the *M2* phase has been achieved [25]. In this case various amounts of W for Mo, Ti for V, Nb for Mo and V, Fe for V and Ce for Te were successfully substituted [25]. The partial replacement of V by Ti was shown to give a significant increase in the specific activity for propene ammoxidation, without affecting the acrylonitrile and acrolein selectivity. The substitution in the same time of Ce for 30% of Te gave increased activity and improved selectivity to acrylonitrile at the expense of acrolein [25].

In this paper, we will report on the attempt to incorporate several element cations (Ge, Sn, Ti W, Mn and Re) in the structure of the *M1* containing Te phase and the study of their effect on the structure and catalytic properties in propane oxidation. The replacement metals were selected considering their valence, coordination and size, chosen to match those of the replaced metals (Table 1). The pure and substituted *M1* phases have been characterized with chemical analysis, BET, XRD, and high-resolution electron microscopy with EDX analyses in order to determine the success of the substitution and they have been tested as catalysts.

2. Experimental

2.1. Catalysts preparation

Non-substituted *M1* phase has been synthesized using the slurry method previously described [19]. This method consisted in preparing an aqueous slurry containing the metal precursors and evaporating it to dryness at 423 K. These precursors were ammonium heptamolybdate and metavanadate, telluric acid and oxalato-niobate in proportion leading to the ratio: Mo/V/Te/Nb = 1/0.27/0.16/0.14. The solid obtained were then successively calcined at 573 K under air for 4 h and at 873 K under nitrogen for 2 h to lead to phases mixtures of *M1* and *M2* phases. The dissolution of the *M2* phases was performed at 333 K by washing the solids in an 3% H_2O_2 aqueous hydrogen peroxide solution, while stirring for 3 h. The remaining solids were finally washed in water, dried at 383 K and re-heated in nitrogen atmosphere at 673 K during 2 h.

The substituted *M1* phases were prepared by the same way except that 5% of the cations Mo, V and Nb were substituted by another element A (Mo/V/Te/Nb/A = 1/0.27/0.17/0.14/0.07). Various precursors have been studied for the A elements but the best results were obtained using $(NH_4)_2WO_4$, NH_4ReO_4, NH_4MnO_4, GeO_2, $TiO_2{\cdot}2H_2O$ and $SnO_2{\cdot}2H_2O$. These precursors were all commercial except $SnO_2{\cdot}2H_2O$, which was prepared by basic hydrolysis of $SnCl_4$ and NH_4MnO_4, which was prepared by reacting $AgMnO_4$, with NH_4Cl as described in the literature [26] and $TiO_2{\cdot}2H_2O$, which was prepared by hydrolyzing $Ti(BuO)_4$. For the W, Ge and Sn, the way the different precursors were mixed and the temperature of addition were key parameters to get a slurry similar to the one obtained in the synthesis of non-substituted *M1* phase. The W and Ge precursors are not readily soluble and have to be added to the solution containing the Mo, V and Te precursors while keeping this solution under boiling. Concerning the Sn and Ti precursors, it is mandatory to add them to the niobium oxalate solution into which they can be dissolved.

M1 phases substituted with Ti and W have also been synthesized with a higher A content (Mo/V/Te/Nb/A = 1/0.27/0.1 > 7/0.14/0.15) either with the same protocol or from an aqueous solution of ammonium heptamolybdate, $(NH_4)_6Mo_7O_{24}{\cdot}4H_2O$, $VOSO_4{\cdot}nH_2O$, TeO_2 and the Ti and W precursors, treated under hydrothermal conditions. In the later case, the reaction was conducted at 448 K for 48 h and the solids produced were filtered and washed thoroughly with distilled water, followed by drying in air at 383 K overnight. The solids were finally treated at 873 K under nitrogen for 2 h.

2.2. Catalysts characterization

The metal contents of the catalysts were determined by atomic absorption (ICP) in an Argon plasma. The spectrometer was a SPECTROLAME-ICP, from SPECTRO. The solids (10 mg) were first solubilized in an aqueous solution (100 ml) containing HF (5 ml) H_2SO_4 (5 ml) and HNO_3 (5 ml) at 473 K under stirring for 6 h. The solution was then vaporized in the plasma and the emission intensity of a radiation characteristic of the element to analyze measured.

The specific surface areas were measured by the BET method with liquid nitrogen adsorption and crystal structures of the pure *M1* phase and the substituted phases were controlled by X-ray diffraction using a BRUKER D5005 diffractometer JEOL 2010 and Cu$K\alpha$ radiation ($\lambda = 1.54184$ Å). The $M1/(M1 + M2)$ ratio in the phase mixtures have been evaluated by comparison of the relative surface areas of the peaks at 30.5° 2θ (*M1* phase) and 36.0° 2θ (*M2* phase) in the X-ray diffraction powder patterns [21]. The method has been validated from results of the fit of a biphasic reference sample using the Rietveld method.

High-resolution electron microscopy was performed with a JEM 2010 (Cs = 0.5 mm). Accelerating voltage was 200 kV with a LaB_6 emission current, a point resolution of 0.195 nm and a useful limit of information of 0.14 nm. The instrument was equipped with an EDS LINK-ISIS (spatial resolution: 1 nm). EDX determinations have been done considering at least 15 analyses.

V *K*-edge XANES spectra were collected at the BM31 beamline at the European Synchrotron Radiation Facility (ESRF) in Grenoble, France. They were recorded at room temperature in the range 5420–5600 eV. The analysis of spectra was based on the observations of the pre-edge. The position of the center of mass and of the total area of V pre-edge peak, were calculated using the PeakFit program and used to determine the mean oxidation state of V. The energy was calibrated with pure metal V foils and several references phases were studied to ensure the analyses as previously described [12]. The Raman spectra were achieved with a LabRam HR spectrometer (Jobin Yvon) equipped with a CCD detector cooled at 77 K. The exciting line at 514.53 nm of an Ar^+–Kr^+ ion laser (Spectra Physics, Model 2018 RM) was focused in the upper part of aqueous solutions using a X50 long working distance objective with a power of 4 mW. For the filtered solids, a X100 objective was used and the laser power was limited to 0.4 mW to avoid laser heating. The Raman spectrum of a silicon plate was previously achieved to adjust band positions. Both for liquids and solids, the wavenumbers reported in the following were accurate within to 2 cm^{-1}. ^{51}V high-resolution NMR spectra were acquired on a Brüker Avance250 at a frequency of 65.77 MHz spectrometer with a 10 mm multinuclear probe. Chemical shifts are referenced on $VOCl_3$ as a standard. Spectral width of 1000 ppm, 512 scans and a pulse length of 2 ms (p/8) are used as acquisition parameters. Spectra processing is done with an exponential line broadening of 15 Hz.

2.3. Oxidation of propane

The oxidation of propane was performed in a fixed bed reactor operating at atmospheric pressure. The apparatus and the conditions have been described elsewhere [21]. The catalytic properties were determined between 593 and 673 K with a catalyst amount varying from 0.1 to 1 g. The feedstock composition was $O_2/C_3H_8/N_2/H_2O = 10/5/40/45$ with a total flow of 30 mL min^{-1}. The gas products and reactants were analyzed on line by gas chromatograph using Porapak-Q and CP-Molsieve 5 Å columns and the organic substrates, condensed and analyzed off line [15]. The catalytic tests were conducted for at least 12 h and the catalysts were recovered after catalytic test by cooling them down in a flow of nitrogen from 673 K.

3. Results

All the catalysts substituted with tetravalent cations (Ti, Sn and Ge) contained only two phases corresponding to *M1* and *M2* as the non-substituted catalyst (Fig. 2a). The $M1/(M1+M2)$ phase ratios determined from X-ray diffraction data were equal to 0.80, 0.84 and 0.83 respectively for the Ge, Ti and Sn substituted solids, and comparable to that of the non-substituted one (0.82). For these catalysts pure *M1* phases were obtained after washing of the *M2* phase as shown in Fig. 2b. This was not the case for all the catalysts substituted with higher valence cations (Fig. 3). The catalyst substituted with W contained well the *M1* and *M2* phases ($M1/(M1+M2) = 0.81$) but the catalysts substituted with Re and Mn did not show any *M1* phase and MoO_3, *M2* and Mo_5O_{14} type phases could be identified. The catalyst substituted with W was washed and a monophasic *M1*(W) phase was obtained. As a consequence the further characterization of the samples and the catalytic testing have been limited to the *M1* phases substituted with Ge, Ti, Sn and W.

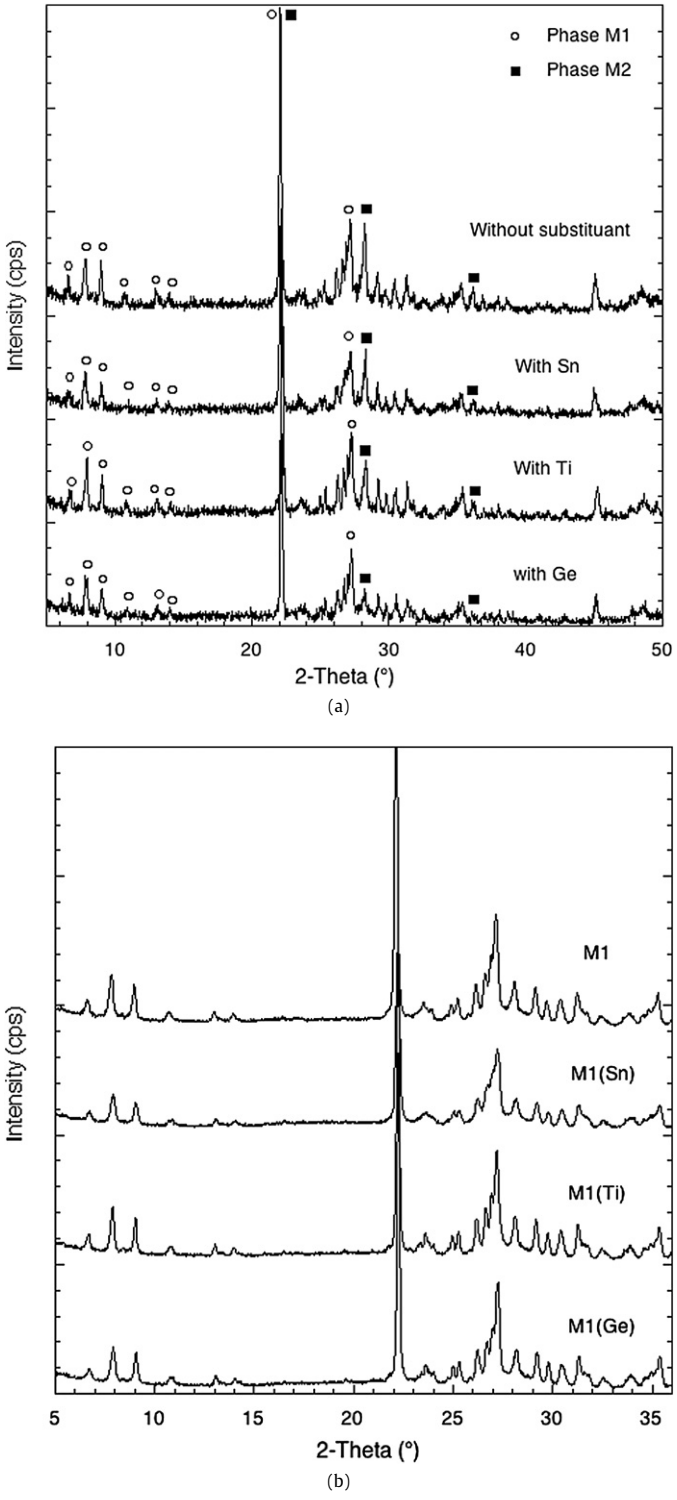

Fig. 2. X-ray diffraction patterns of the catalysts non-substituted and substituted with tetravalent cations (a) and of the corresponding *M1* phases obtained after washing (b).

For the later phases, the mass balances of the dissolutions have been calculated. The results obtained were in good agreement with the $M1/(M1+M2)$ phase ratios calculated from XRD data, which showed that only *M2* phases were dissolved.

The cell parameters of the later compounds have been calculated as well as their specific surface area (Table 2). No signifi-

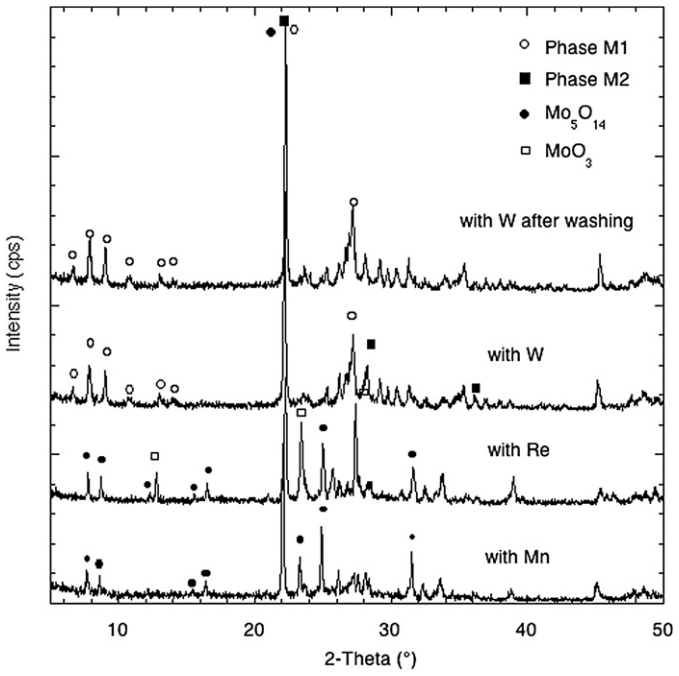

Fig. 3. X-ray diffraction patterns of the catalysts substituted with W, Re and Mn and of the catalysts substituted with W after washing.

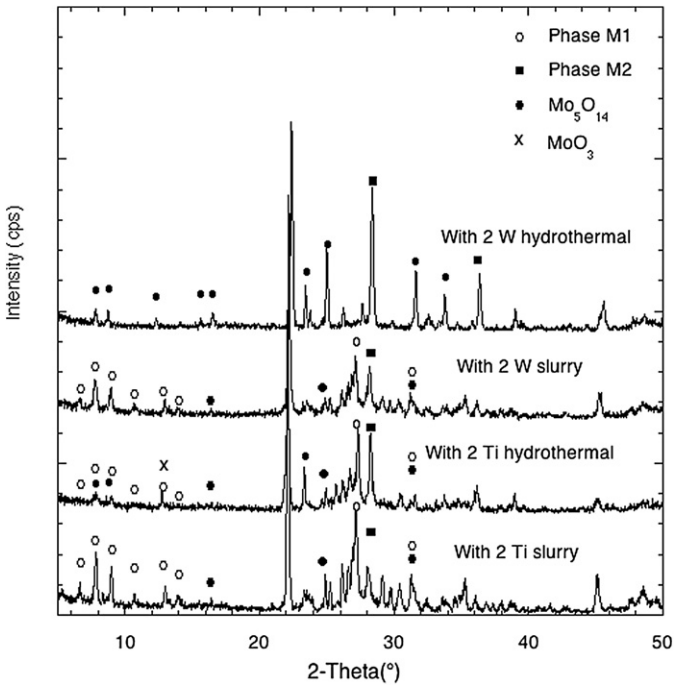

Fig. 4. X-ray diffraction patterns of the catalysts substituted with twice the amount of W (2 W) and Ti (2 Ti) and prepared using the slurry and the hydrothermal method.

Table 2
Unit cell parameters of the *M1* phase with different substituting elements and their specific surface area measured using the BET method.

Catalyst	*a* (nm)	*b* (nm)	*c* (nm)	S_{BET} ($m^2\,g^{-1}$)
M1(Ge)	2.103(1)	2.668(1)	0.4013(3)	22.0
M1(Ti)	2.101(2)	2.671(2)	0.4012(2)	18.8
M1(Sn)	2.102(3)	2.669(3)	0.4014(7)	30.9
M1(W)	2.1016(9)	2.6688(9)	0.4012(1)	29.1
M1	2.1033(5)	2.670(1)	0.4013(1)	23.0

Table 3
Chemical composition of the unit cell of the *M1* phases calculated from the chemical analyses and the EDX analyses.

Solid	Unit cell composition				
	Substituting element	Mo	V	Nb	Te
M1(Ge)					
Chem. an.	–	13.8	3.9	2.3	1.1
EDX	–	14.4	3.5	2.1	1.1
M1(Ti)					
Chem. an.	1.1	13.5	3.5	1.9	1.2
EDX	0.6	14.6	3.2	1.6	1.4
M1(Sn)					
Chem. an.	0.7	13.7	3.6	2.0	1.2
EDX	0.4	14.7	3.2	1.7	1.1
M1(W)					
Chem. an.	1.1	13.3	3.6	2.0	1.2
EDX	0.9	13.9	3.3	1.8	1.2
M1					
Chem. an.	–	14.2	3.7	2.1	1.3
EDX	–	14.7	3.3	2.0	1.1

cant variation of cell parameters was observed for the substituted compounds and all the cell parameters were close to those published for the *M1* phase (Pba2-No. 32 with $a = 2.1134(2)$ nm, $b = 2.6658(2)$ nm, $c = 0.40146(3)$ nm) [13]. The surface areas of the substituted compounds were comparable, except that of *M1*(Sn) and *M1*(W) which were higher.

The chemical analyses of the *M1* phases after washing are presented in Table 3. The substituting element content of the *M1* phase corresponded to that of the starting formula for *M1*(Ti) and *M1*(W), which lead to the conclusion that Ti and W have equivalently been distributed between the two phases *M1* and *M2* during the synthesis process. The content is lower for *M1*(Sn) and there was no Ge in the *M1*(Ge) phase. The V and Nb content of the compounds were comparable to each other and to that of the non-substituted phase except for the *M1*(Ge) compound which contained more V and Nb. No significant variation of Te content was ever observed. The *M1* phase have also been characterized by high-resolution electron microscopy with EDX analyses. The images obtained for the phases were very similar showing that no specific texture was developed with the substitution. In parallel, the EDX analyses showed that no *M2* particles, which have a composition very different from that of the *M1* phase were detectable. Furthermore they confirmed the results of the chemical analyses (Table 3). In particular they showed that no Ge was introduced in the *M1* structure; in all the analyses of the *M1*(Ge) phase, Ge was never present and the V content of the *M1*(Ge) phase was systematically higher. The EDX analyses showed Mo contents systematically slightly higher than the chemical analyses and substituting elements contents lower.

The very low Sn content of the *M1*(Sn) compared to the starting content led to the conclusion that the limit of solid solution of Sn in the *M1* structure has been reached. However the limit of solubility of Ti and W in the *M1*(Te) phase may not be reached and that the *M1* phase could contain more Ti or W. In order to check if in these cases the limits of the solid solutions had been reached, syntheses with higher substituting element contents have been performed. In the same time, hydrothermal syntheses of the same compounds were made to also check if the preparation method could have an effect on the phases obtained. The X-ray diffraction patterns of the prepared solids are shown in Fig. 4. It can be seen that whatever the preparation method the solids with higher substituent contents contained besides the *M1* and *M2* phases other phases like MoO_3 and Mo_5O_{14} type phase, which are insoluble and

Table 4
Comparison of the catalytic performances of the *M1* phases substituted with Ge, Ti, Sn and W with those of an undoped *M1* phase.

Solid	Mass (mg)	*T* (K)	Conv. (%)	Prop. conv. rate (10^{-8} mol $s^{-1} g^{-1}$)	Selectivity (%)					
					CO_x	C_3H_6	Acet	AA	ProA	AcrA
M1(Ge)	100	596	10.5	5.38	11	20	1	11	1	56
		629	19.4	10.23	26	14	0	12	0	48
		661	35.0	18.46	38	9	0	13	0	40
M1(Ti)	228	598	9.7	2.52	23	20	1	14	1	41
		632	16.8	4.37	34	16	0	17	0	33
		661	24.9	6.48	46	13	0	16	0	25
M1(Sn)	164	597	10.8	2.37	22	17	1	13	1	46
		632	20.7	4.55	32	13	0	15	0	40
		664	32.8	7.22	48	9	0	14	0	29
M1(W)	107	597	9.8	3.51	16	23	1	10	2	48
		632	19.1	6.48	27	16	0	15	1	41
		665	33.3	11.93	38	11	0	14	0	37
M1	155	597	10.4	3.26	14	20	1	11	1	53
		632	20.1	6.30	27	14	0	13	0	46
		665	35.7	11.19	38	9	0	13	0	40

Note. Prop. conv. rate = propane conversion rate, Acet = acetone, AA = acetic acid, ProA = propionic acid, AcrA = acrylic acid. Total flow rate: 30 mL min^{-1}, composition $C_3H_8/O_2/N_2/H_2O = 5/10/40/45$.

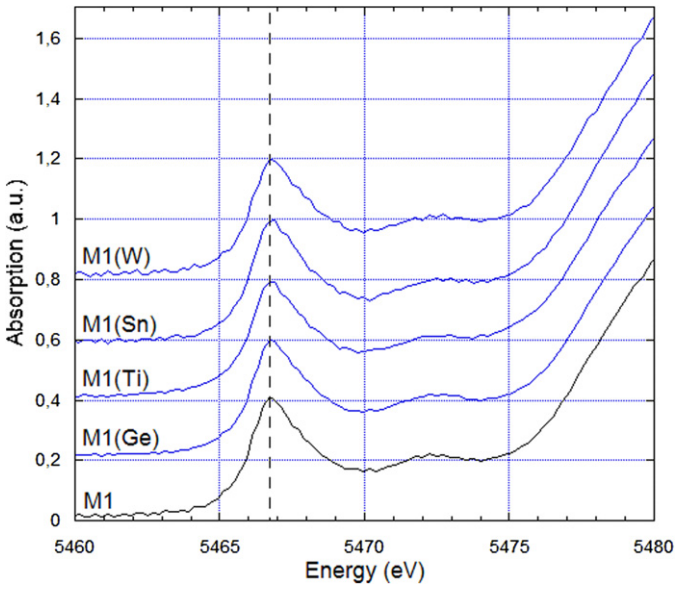

Fig. 5. XANES spectra at V *K*-edge of the pure and substituted *M1* phases.

inactive or unselective. For the W substituted solids, the hydrothermal method appeared worse than the slurry method since almost no *M1* phase was obtained at high W content. From this study, it can thus be concluded that the limit of solid solution of Ti and W in the *M1* structure should lie between 5 and 10% in terms of the Mo + V + Nb + A cations.

The catalytic performances of the substituted *M1* phases have been compared at different temperatures to those of the non-substituted one (Table 4). Taking into account the masses of catalysts tested, their specific surface areas and the obtained conversions, it can easily be concluded that the *M1*(W) activity is rather similar to that of pure *M1*, it is lower for *M1*(Ti) and *M1*(Sn) and higher for *M1*(Ge). Comparing catalysts at iso-conversion, the same conclusion can be drawn concerning the selectivity to acrylic acid. *M1*(W), *M1*(Ti) and *M1*(Sn) were less selective contrarily to *M1*(Ge) which is slightly more selective. This positive effect on the selectivity in acrylic acid, however tend to disappear at higher reaction temperature. The apparent activation energies were comparable for the pure phase, *M1*(W) and *M1*(Ge) with 60, 59 and 61 kJ mol^{-1}, but significantly lower for *M1*(Ti) and *M1*(Sn) with 49 and 54 kJ mol^{-1}.

Finally, XANES spectra at V *K*-edge of the pure and substituted *M1* phases have been recorded (Fig. 5). All the spectra are remarkably similar and show a constant mean oxidation state of 4.1 for the vanadium. Since the V^{5+}/V^{4+} redox couple is reasonably the first redox couple that would be affected by an oxido-reduction modification of the solid catalyst [27], it can be concluded that the substitution did not change significantly the charge distribution in the structure.

4. Discussion

Prior to discussing the results obtained, a brief summary of the description that has been hypothesized for the catalytic active site at the surface of the *M1* phase is proposed: It is now commonly accepted that the active centers of *M1* are located on the surface of its basal plane (001) and contain all needed key catalytic functionalities properly arranged within bonding distance of each other to convert propane directly to nitrile or acid. The structure of the *M1* phase along this plane is presented in Fig. 1. For clarity, the same nomenclature for the different sites as that used for the description of the structure in the different structure determination studies has been kept.

It has been proposed that in these planes the paraffin-activating site was V^{5+} site (*M7*) located along heptagonal channel. The Te^{4+} site located nearby in the hexagonal channel would be the α-H abstracting site whereas the Mo^{6+} sites (*M4*, *M5*) the oxygen (NH) inserting site and the acid (acrylonitrile) finishing site [27]. The pentagonal channels occupied by Nb cations lead in the (001) plane to {(Nb)Mo5} arrangements which delineate each active center and separate them spatially from each other.

The Te^{4+} sites in the hexagonal channels are key to the α-H abstraction of the intermediates in the oxidation of propane like are other cations with lone pair electrons (Bi, Sb) in general in other oxidation reactions [28]. It is why the substitution attempted only concerned the cations in the octahedral network.

The results obtained with all the cations showed that the substitutions were very limited and less than 1 per 10 cations in the octahedral network. Although it is not a lot, the substitutions appeared to have significant effects on the catalytic properties of the solids.

The catalytic data obtained with the solids *M1*(W) showed no change in catalytic activity but a small decrease in acrylic acid selectivity (Table 4). It is rather evident that W^{6+} cations substitute Mo^{6+} cations. However since the W^{6+}/W^{5+} redox couple is deeper than the Mo^{6+}/Mo^{5+} one, Mo should preferentially be reduced and consequently the W cations should occupy the sites specific to Mo^{6+}: *M5*, *M6*, *M8*, *M10* and *M11* constituting the {(Nb)Mo5} columns and eventually the sites *M3* and *M7*, which are only partially occupied by Mo^{6+}. None of these sites are directly involved in the catalytic reaction except the site *M7* and *M5*. The first one, which is the site responsible for the activation of the alkane and which determines the catalyst activity since this activation is the rate-limiting step of the total reaction, is involved only when occupied by V. It is therefore understandable that W cations had no effect on the catalytic activity and that the apparent activation energy for the transformation of propane remained the same for pure *M1* and *M1*(W). Furthermore the substitution of Mo by W in the *M7* site, if it takes place, apparently does not modify the V content of the site. The second site (*M5*) is the oxygen inserting site and acid finishing site. The occupation of this site by inactive W would decrease the selectivity to acrylic acid to the benefit of that in propene, which cannot be further transformed. This is indeed

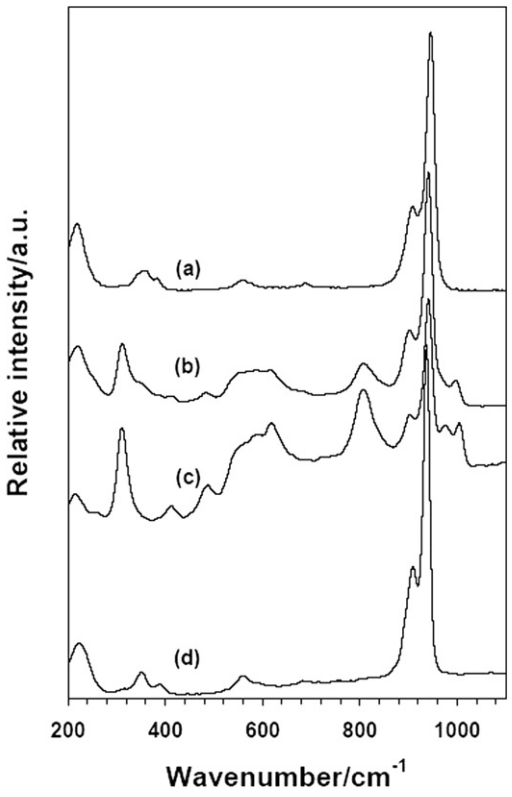

Fig. 6. Raman spectra of the solution with Mo + Te precursors (a), the solution with Mo + Te + V precursors (b), the solution with Mo + V + Te + Ge precursors (c) and of the solid precipitated from the solution with Mo + V + Te + Ge precursors (solid) (d).

what is observed. The catalytic data obtained show that W substitution slightly lowers the selectivity to acrylic acid mainly to the benefit of that in propene.

Ti and Sn cations had a negative effect both on the selectivity and the activity (Table 4). They are tetravalent cations and they should substitute preferentially for V^{4+} or possibly V^{5+} or Mo^{5+}. These substitutions would occur on the different sites occupied by these cations i.e *M1*, *M2*, *M3*, *M4*, *M5* and *M7*. The *M3* and *M1* sites correspond to isolated sites connecting respectively hexagonal to heptagonal channels and heptagonal channels together. They have no specific catalytic role and with the most distorted oxygen environment, should accept with more difficulties cations like Sn and Ti, which are larger (Table 1). The remaining sites correspond to catalytic sites (*M5*, *M7*) or to sites neighboring the catalytic sites (*M2*). The substitution on the first sites by Ti^{4+} and Sn^{4+} will directly lower the number of these sites and consequently the activity and the selectivity of the catalyst, whereas the substitution on the later may modify the *M7* site responsible for the activation, which could explain why the activity and the apparent activation energy are decreasing.

The effect of Ge is more difficult to understand because it did not enter at all the structure of the *M1* phase. It had however a significant effect on both the activity and the selectivity (Table 4).

In order to try to elucidate the origin of the effect of Ge on the composition of the phases, Raman and ^{51}V NMR spectra of the starting solution for the preparation of the slurry have been recorded at different steps of metallic precursors addition (Figs. 6 and 7). The stoichiometry of the aqueous solution as well as its concentration was kept similar to that given in the experimental section and corresponded exactly to a standard solid preparation. Upon addition of telluric acid to the ammonium heptamolybdate solution, Anderson-type anions $(TeMo_6O_{24})^{6-}$ characterized by bands at 944, 907 cm^{-1} ν(Mo=O) and 683 cm^{-1} ν(Te–O–Mo)

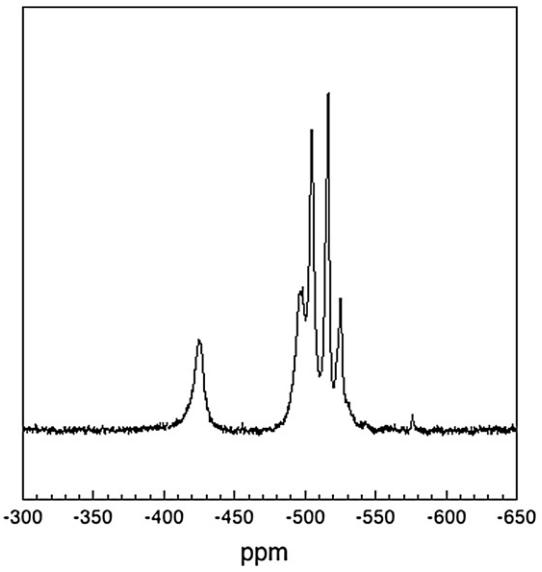

Fig. 7. ^{51}V NRM spectrum of the solution with Mo + Te + V precursors.

were formed (Fig. 6a). The remaining experimental frequencies at 560, 352 and 222 cm^{-1} were respectively assigned to asymmetric stretchings of Te–O and bendings of Mo–O–Mo bonds [29].

When vanadium was then added to the solution, its color became orange and then turned red. The Raman spectrum of the obtained solution was quite different (Fig 6b). It still contained bands corresponding to Anderson-type anions but other bands corresponding to V=O (997 cm^{-1}) and to V–O–M (M = V, Mo) stretching vibrations (550, 580, 615, 810 cm^{-1}). The new species have been identified by ^{51}V NMR spectroscopy. The ^{51}V NMR spectrum of the solution clearly showed the presence of $V_9MoO_{28}^{5-}$ species or their protonated forms to which resonances with chemical shifts (δ/ppm) −424.65, −498.44, −504.97, −516.75 and −525.48 are associated [30] (Fig. 7). The presence of non-substituted $V_{10}O_{26}^{6-}$ species that can be characterized by resonances with chemical shifts (δ/ppm) −424.65, −498.44, and −516.75, may also be present [31]. The peaks with low intensity at −498.4 and −576.2 could respectively be attributed to the presence of $V_2Mo_4O_{19}^{4-}$ and $(VO_3^-)_x$ species in very small amount. The presence of the $V_{10}O_{26}^{6-}$ type species was normal since they are the stable vanadium species in water in the conditions of pH and concentration used. Upon addition of Ge, the Raman spectrum remained almost the same except for the appearance of new bands at 974, 619 and 405 cm^{-1} (Fig. 6c). These new bands can be attributed to the presence of Keggin-type $(GeMo_{12}O_{40})^{4-}$ species [32]. With time the solution became cloudy. The precipitate formed has been separated by filtration. Its Raman spectrum corresponded to an Anderson-type salt $(NH_4)_6TeMo_{12}O_{40}{\cdot}xH_2O$ [33] (Fig. 6d). The formation of the Keggin-type species or the Anderson salt led to a segregation of molybdenum in or out of the solution, which changed in composition or got richer in vanadium. This could explain the formation from the solution of a *M1* phase richer in vanadium. As a consequence of this enrichment, the V occupancy of the sites shared by V and Mo cations in the *M1* structure was higher. This was the case of the *M7* sites and since these sites when occupied by V are activating propane, the catalyst activity was higher. The sites remained the same and this is in agreement with the non-variation of the apparent activation energy but they simply increased in number. Interestingly, the selectivity to acrylic acid also increased but more slightly. This may be due to the increase of the V occupancy of the other neighboring V containing sites that may indirectly modify the catalytic properties of the catalytic sites. A recent structure analysis of the *M1* phase reports that V can very partially occupy

the *M4* and *M5* sites [34]. It may thus also be hypothesized that V content of these sites would increase and this would have a positive effect on their catalytic efficiency.

5. Conclusion

The results obtained showed that substitutions of cations in the octahedral network of the *M1* phase were possible although very limited. *M1* phases containing Ti, Sn and W cations have been obtained but with limit of solid solutions, which did not exceed 10% in cations. Attempts to introduce Ge, Mn or Re in the structure have failed. However if only *M2* or Mo_5O_{14} type phases were obtained with Mn and Re, *M1* and *M2* phase mixtures similar to those obtained without substituting elements were formed when Ge was present in the starting slurry. XANES spectroscopy at V K-edge showed no change in oxidation state of vanadium, which tend to show that mainly isovalent substitutions were taking place. This is confirmed by chemical analysis for *M1*(W) but not *M1*(Ti) and *M1*(Sn).

The study of the catalytic properties of the substituted *M1* phase showed that (i) W had no effect on the activity but slightly decreased the selectivity to acrylic acid, (ii) the introduction of Ti and Sn decreased both the activity and the selectivity to acrylic acid and (iii) the addition of Ge in the slurry although not present in the final *M1* phase, increased strongly the activity and to a lesser extent the selectivity to acrylic acid. This indirect effect has been related to the vanadium content of the *M1* phase, which increased in comparison with the pure *M1* phase. The alkane-activating site has been proposed to correspond to a V occupying a given crystallographic site (*M7*). This site being shared by V and Mo cations, we proposed that the increase of vanadium content of the phase would lead to a higher occupancy of this site by V and consequently to more active sites. This observation tends to show that there is a track of improvement in finding a preparation method for the catalyst allowing to increase the vanadium content in the *M1* phase at the expense of Mo. Otherwise none of the substitution attempted led to an improvement of the catalyst efficiency.

Acknowledgments

The authors would like to thank Dr. Carmelo Prestipino local contact of beamline BM31 at the European Synchrotron Radiation Facility (ESRF) in Grenoble (France) who provided help and support in the recording of XANES spectra.

References

[1] M. Hatano, A. Kayo, US patent 5,049,692 (1991), to Mitsubishi Kasei Co.
[2] T. Ushikubo, K. Oshima, A. Kayou, M. Hatano, Stud. Surf. Sci. Catal. 112 (1997) 473.
[3] P. Botella, J.M. Lopez Nieto, B. Solsona, A. Misfud, F. Marquez, J. Catal. 209 (2002) 445.
[4] J.M.M. Millet, M. Baca, A. Pigamo, D. Vitry, W. Ueda, J.L. Dubois, Appl. Catal. A 244 (2003) 359.
[5] P. DeSanto Jr., D.J. Buttrey, R.K. Grasselli, C.G. Lugmair, A.F. Volpe, B.H. Toby, T. Vogt, Top. Catal. 23 (2003) 23.
[6] N.R. Shiju, X. Liang, A.W. Weimer, C. Liang, S. Dai, V.V. Guliants, J. Am. Chem. Soc. 130 (18) (2008) 5850.
[7] T. Ushikubo, K. Oshima, A. Kayou, M. Hatano, Stud. Surf. Sci. Catal. 112 (1997) 473.
[8] T. Ushikubo, K. Oshima, A. Kayou, M. Vaarkamp, M. Hatano, J. Catal. 169 (1997) 394.
[9] M. Lin, T. Desai, F. Kaiser, P. Klugherz, Catal. Today 61 (2000) 223.
[10] R. Fushimi, S.O. Shekhtman, A. Gaffney, S. Han, G.S. Yablonsky, J.T. Gleaves, Ind. Eng. Chem. Res. 44 (16) (2005) 6310.
[11] N. Shiju, K. Raveendran, R. Ramesh, S.S. Iyer, V.V. Guliants, J. Phys. Chem. C 111 (49) (2007) 18001.
[12] M. Baca, J.M.M. Millet, Appl. Catal. A 279 (2005) 67.
[13] P. De Santo, J. Buttrey, R.K. Grasselli, C.G. Lugmair, A.F. Volpe, B.H. Togy, T. Vogt, Z. Kristallogr. 219 (2004) 152.
[14] O.V. Safonova, B. Deniau, J.M.M. Millet, J. Phys. Chem. B 110 (2006) 236962.
[15] W. Ueda, K. Oshihara, D. Vitry, T. Hisano, Y. Kayashima, Catal. Surv. Jpn. 6 (1/2) (2002) 33.
[16] M. Sadakane, N. Watanabe, T. Katou, Y. Nodasaka, W. Ueda, Angew. Chem. Int. Ed. 46 (2007) 1493.
[17] P. Botella, E. García-González, A. Dejoz, J.M. López Nieto, M.I. Vázquez, J. González-Calbet, J. Catal. 225 (2004) 428.
[18] J.M. López Nieto, P. Botella, P. Concepción, A. Dejoz, M.I. Vázquez, Catal. Today 91–92 (2004) 241.
[19] W.C. Zhu, M.J. Jia, Z.L. Wang, G.J. Wang, T.H. Wu, Gaodeng Xuexiao Huaxue Xuebao 28 (2) (2007) 334.
[20] J. Holmberg, R.K. Grasselli, A. Andersson, Top. Catal. 23 (2003) 55.
[21] M. Baca, M. Aouine, J.L. Dubois, J.M.M. Millet, J. Catal. 233 (2005) 234.
[22] T. Ushikubo, K. Oshima, T. Ihara, H. Amatsu, US Patent 5,534,650 (1996), assigned to Mitsubishi Chemical Co.
[23] H. Hibst, F. Rosowski, G. Cox, Catal. Today 117 (2006) 234.
[24] N.R. Shiju, V.V. Guliants, Prep.-Am. Chem. Soc. Div. Pet. Chem. 52 (1) (2007).
[25] J. Holmberg, S. Hansen, R.K. Grasselli, A. Andersson, Top. Catal. 38 (2006) 17.
[26] C.T. Odin, Z. Anorg. Chem. 24 (1900) 203.
[27] R.K. Grasselli, D.J. Buttrey, J.D. Burrington, A. Andersson, J. Holmberg, W. Ueda, J. Kubo, C.G. Lugmair, A.F. Volpe Jr., Top. Catal. 38 (1–3) (2006) 7.
[28] R.K. Grasselli, Top. Catal. 15 (2001) 93.
[29] R. Grabowski, A. Gumula, J. Aloczynski, J. Phys. Chem. Solids 41 (1980) 1027.
[30] R.I. Maksimovskaya, N.N. Chumachenko, Polyhedron 6 (10) (1987) 1813.
[31] H.T. Evans, Perspect. Struct. Chem. 4 (1971) 1.
[32] C. Rocchiccioli-Deltcheff, R. Thouvenot, R. Franck, Spectrochim. Acta A 32 (1976) 587.
[33] I.L. Botto, C.I. Cabello, H.J. Thomas, Mater. Chem. Phys. 47 (1997) 37.
[34] H. Murayama, D. Vitry, W. Ueda, G. Fuchs, M. Anne, J.L. Dubois, Appl. Catal. A 318 (2007) 137.